

# Synthesis, Structures and Properties of Cluster Complexes [H<sub>3</sub>O(Ph<sub>3</sub>PO)<sub>3</sub>]<sub>2</sub>[Mo<sub>6</sub>Cl<sub>14</sub>] and [H(Ph<sub>3</sub>PO)<sub>2</sub>]<sub>2</sub>[Re<sub>6</sub>S<sub>6</sub>Br<sub>8</sub>]

Zhyldyz S. Kozhomuratova,<sup>[a]</sup> Yuri V. Mironov,<sup>[a]</sup> Michael A. Shestopalov,<sup>[a]</sup>  
Irina V. Drebuschak,<sup>[a]</sup> Nikolay K. Moroz,<sup>[a]</sup> Dmitry Y. Naumov,<sup>[a]</sup> Anton I. Smolentsev,<sup>[a]</sup>  
Evgenii M. Uskov,<sup>[a]</sup> and Vladimir E. Fedorov\*<sup>[a]</sup>

**Keywords:** Cluster compounds / Molybdenum / Rhenium / Triphenylphosphane oxide / Crystal structure / NMR spectroscopy / Hydrogen bonding

New cluster compounds [H<sub>3</sub>O(Ph<sub>3</sub>PO)<sub>3</sub>]<sub>2</sub>[Mo<sub>6</sub>Cl<sub>14</sub>] (**I**) and [H(Ph<sub>3</sub>PO)<sub>2</sub>]<sub>2</sub>[Re<sub>6</sub>S<sub>6</sub>Br<sub>8</sub>] (**II**) have been prepared by the reaction of a acetonitrile solution of triphenylphosphane oxide Ph<sub>3</sub>PO with octahedral cluster complexes of molybdenum (H<sub>3</sub>O)<sub>2</sub>Mo<sub>6</sub>Cl<sub>14</sub>·6H<sub>2</sub>O and rhenium K<sub>2</sub>Re<sub>6</sub>S<sub>6</sub>Br<sub>8</sub>, respectively, (with addition of several drops of HBr). The structures and properties of the products were studied by single-crystal

X-ray diffraction and NMR and luminescence spectroscopic methods. The compounds studied are characterized by strong hydrogen bonds with O–O distances of 2.45–2.51 Å (**I**) and 2.34–2.41 Å (**II**); unusual H-bonded cationic trimers, [H<sub>3</sub>O(Ph<sub>3</sub>PO)<sub>3</sub>]<sup>+</sup>, were found in compound **I**.  
(© Wiley-VCH Verlag GmbH & Co. KGaA, 69451 Weinheim, Germany, 2007)

## Introduction

The reactions of triphenylphosphane oxide (Ph<sub>3</sub>PO) with various acids give molecular compounds of different types. Compounds with the stoichiometry Ph<sub>3</sub>PO/acid = 1:1 are formed for the reactions with HNO<sub>3</sub>,<sup>[1]</sup> HF,<sup>[2]</sup> HCl,<sup>[3]</sup> HBr,<sup>[4]</sup> CCl<sub>3</sub>COOH.<sup>[5]</sup> Compounds with a Ph<sub>3</sub>PO/acid ratio of 2:1 are also found – (Ph<sub>3</sub>PO)<sub>2</sub>·H<sub>2</sub>O·HBr,<sup>[6]</sup> (Ph<sub>3</sub>PO)<sub>2</sub>·(CH<sub>3</sub>)<sub>2</sub>C(COOH),<sup>[7]</sup> (Ph<sub>3</sub>PO)<sub>2</sub>·HAuCl<sub>4</sub>,<sup>[8]</sup> (Ph<sub>3</sub>PO)<sub>2</sub>·HClO<sub>4</sub>.<sup>[9]</sup> The compounds that form from triphenylphosphane oxide and acids can be separated into three main groups depending on the nature of the interaction between the acidic protons and the Ph<sub>3</sub>PO molecules.<sup>[9]</sup> The first group includes compounds in which the hydrogen atoms belong more to the acid than to the Ph<sub>3</sub>PO molecule, as, for example, in the case of Ph<sub>3</sub>PO·CCl<sub>3</sub>COOH. In such compounds, the lengths of the P=O bonds are close to those observed in the free Ph<sub>3</sub>PO molecule (1.487 Å).<sup>[10]</sup> In the second group, on the contrary, the proton lies more towards Ph<sub>3</sub>PO, which results in a remarkable lengthening of the P=O bond. Such compounds can be considered as ionic pairs (e.g. [Ph<sub>3</sub>POH]<sup>+</sup>Cl<sup>−</sup>), and their formation is typical of non-oxygen acids. The third group combines the compounds in which the Ph<sub>3</sub>PO molecules are bound together by strong symmetrical or non-symmetrical hydrogen bonds, but the anions do not participate in the hydrogen bonding. A typical example of such compounds is (Ph<sub>3</sub>PO)<sub>2</sub>HClO<sub>4</sub>, where the two triphenylphosphane oxide fragments are bound to-

gether by very short (2.41 Å) hydrogen bonds to form a dimer cation [Ph<sub>3</sub>PO...H...OPPh<sub>3</sub>]<sup>+</sup>.<sup>[9]</sup>

The interaction of chloromolybdenic(II) acid (H<sub>3</sub>O)<sub>2</sub>Mo<sub>6</sub>Cl<sub>14</sub> with triphenylphosphane oxide was first studied by Sheldon,<sup>[11]</sup> but the reaction products were not described thoroughly enough and their structure was not studied.

In this paper we present the synthesis of two novel cluster compounds containing Ph<sub>3</sub>PO molecules: [H<sub>3</sub>O(Ph<sub>3</sub>PO)<sub>3</sub>]<sub>2</sub>[Mo<sub>6</sub>Cl<sub>14</sub>] (**I**) and [H(Ph<sub>3</sub>PO)<sub>2</sub>]<sub>2</sub>[Re<sub>6</sub>S<sub>6</sub>Br<sub>8</sub>] (**II**). In the frame of the above classification, these compounds can be assigned to the third group, since their triphenylphosphane oxide molecules are connected by strong hydrogen bonds to form large cationic complexes: dimers [H(Ph<sub>3</sub>PO)<sub>2</sub>]<sup>+</sup> (in **II**) and unusual trimers [H<sub>3</sub>O(Ph<sub>3</sub>PO)<sub>3</sub>]<sup>+</sup> (in **I**). Inspection of the Cambridge crystallographic database showed that the trimeric cation, namely tris(oxotriphenylphosphane)-oxonium, has not been mentioned in the literature so far. Therefore, it is interesting to consider its structure in detail. The structures of the H-bonded complexes **I** and **II** were solved by single-crystal X-ray diffraction and examined by solid-state NMR spectroscopy.

## Results and Discussion

The interaction of the cluster acid (H<sub>3</sub>O)<sub>2</sub>Mo<sub>6</sub>Cl<sub>14</sub> and triphenylphosphane oxide gives a complex compound [H<sub>3</sub>O(Ph<sub>3</sub>PO)<sub>3</sub>]<sub>2</sub>[Mo<sub>6</sub>Cl<sub>14</sub>] (**I**). The unit cell of compound **I** contains one centrosymmetrical and two noncentrosymmetrical [Mo<sub>6</sub>Cl<sub>14</sub>]<sup>2−</sup> anions formed by slightly distorted Mo<sub>6</sub> octahedrons with Mo–Mo distances of 2.594–2.608 Å (Table 1, Figure 1, Figure 2). The lengths of the Mo–Cl

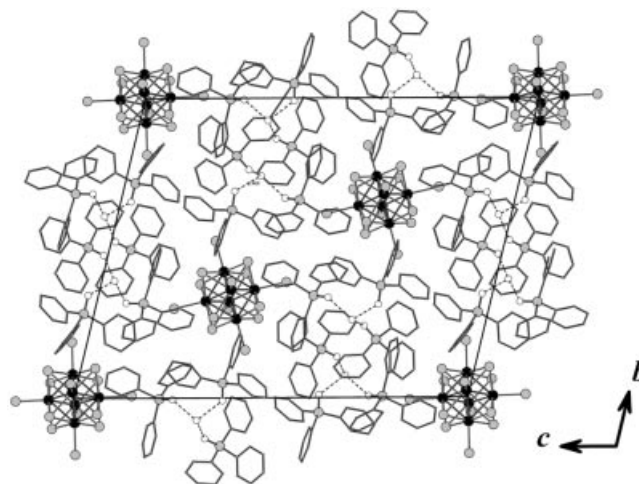
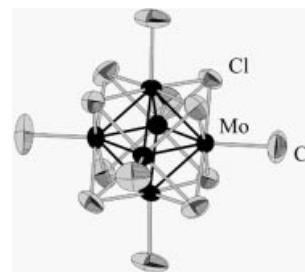
[a] Nikolaev Institute of Inorganic Chemistry, Siberian Branch of Russian Academy of Sciences,  
3, Akad. Lavrentiev prospect, Novosibirsk, 630090, Russia  
E-mail: fed@che.nsk.su

Table 1. Crystallographic data for compounds **I** and **II**.

	<b>I</b>	<b>II</b>
Chemical formula	$C_{108}H_{96}Cl_{14}Mo_6O_8P_6$	$C_{72}H_{62}Br_8O_4P_4Re_6S_6$
Formula weight	2779.61	3063.94
Crystal size [mm]	$0.40 \times 0.40 \times 0.40$	$0.12 \times 0.10 \times 0.08$
Crystal system	triclinic	triclinic
Space group	$P\bar{1}$	$P\bar{1}$
$a$ [Å]	13.5625(10)	13.2357(4)
$b$ [Å]	22.6936(17)	18.1285(6)
$c$ [Å]	29.316(2)	18.7516(6)
$\alpha$ [°]	103.240(2)	94.5280(10)
$\beta$ [°]	99.354(2)	104.9130(10)
$\gamma$ [°]	91.857(2)	105.6660(10)
$V$ [Å <sup>3</sup> ]	8643.4(11)	4132.6(2)
$Z$	3	2
$D_{\text{calcd.}}$ [Mg/m <sup>3</sup> ]	1.602	2.462
Diffractometer	Bruker Nonius X8Apex	Bruker Nonius X8Apex
Temperature [K]	293(2)	298(2)
$\mu$ (Mo- $K\alpha$ ) [mm <sup>-1</sup> ]	1.094	12.894
$\theta$ range for data collection [°]	1.30 to 25.68	1.50 to 28.26
Absorption correction	multiscan (SADABS; Bruker 2004)	multiscan (SADABS; Bruker 2004)
Goodness-of-fit on $F^2$	0.965	0.953
Reflections collected/unique	46022/32128 [ $R_{\text{int}} = 0.0200$ ]	34098/20065 [ $R_{\text{int}} = 0.0431$ ]
Final $R$ indices [ $I > 2\sigma(I)$ ]	$R_1 = 0.0440$ , $wR_2 = 0.0871$	$R_1 = 0.0480$ , $wR_2 = 0.0992$
$R$ indices (all data)	$R_1 = 0.0939$ , $wR_2 = 0.1018$	$R_1 = 0.1054$ , $wR_2 = 0.1132$
$\Delta\rho$ (max; min) [e Å <sup>-3</sup> ]	0.476; -0.710	1.941; -1.558

bonds, 2.421(8) Å and 2.472(5) Å for terminal and bridged ligands, respectively, are typical of those observed in related clusters.<sup>[12–14]</sup> The formation of the unusual cationic complex ion  $[H_3O(Ph_3PO)_3]^+$  (Figure 3) is a distinctive feature of the structure. Such structures consist of three triphenylphosphane oxide molecules that are H-bonded to a central oxygen atom ( $O_W$ ) to form a trigonal pyramid  $\{O_3O_W\}$  (see the inset in Figure 3). The  $O-O_W$  lengths (Table 2) range between 2.449 Å and 2.504 Å, which indicates relatively strong hydrogen bonding. The angles  $O-O_W-O$  are within the range 99.1–110.4°. However, as is evident from Table 2, the H-bonding does not lead to considerable deformation of the  $P=O$  bonds. Relative to unbound  $Ph_3PO$ ,<sup>[10,15]</sup> the bonds are approximately 0.01 Å longer. This fact might be indicative of a shift in the positions of the protons towards the central oxygen atom to form the  $H_3O^+$  ion as a cation–complex core.

We studied the H-bond geometry by <sup>1</sup>H NMR wide-line spectroscopy. The NMR spectrum of the compound **I** (Figure 4) is determined mainly by magnetic dipole–dipole interactions of the  $C_6H_5$  ring protons, whereas the protons involved in the hydrogen bonds, which are closer together and therefore coupled more strongly, are represented as very feeble tails at the absorption edges. In this regard, we considered the spectral domains at frequencies  $|\Delta f| = (25 - 60)$  kHz where the influence of the aromatic protons is not overwhelming. The spectra recorded below 200 K were chosen for analysis since higher temperatures result in significant narrowing of the NMR spectra because of increased proton mobility. The simulation of the spectrum was performed by an approach outlined in the Experimental Section. The best fits to the experimental spectra were obtained for a three-spin configuration close to equilateral (the distortion of the triangle sides does not exceed 2%), with an

Figure 1. Packing in the crystal structure of  $[H_3O(OPPh_3)_3]_2-[Mo_6Cl_{14}]$ .Figure 2. The structure of the cluster anion  $[Mo_6Cl_{14}]^{2-}$  in compound **I**. Displacement ellipsoids are drawn at the 50% probability level.

average proton–proton distance of 1.76(1) Å. On the basis of these assessments and by supposing the linearity of the

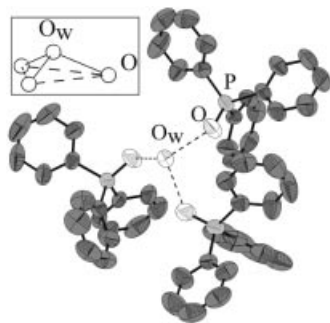


Figure 3. The structure of the cation  $[\text{H}_3\text{O}(\text{OPPh}_3\text{O})_3]^+$  in compound **I**. Displacement ellipsoids are drawn at the 50% probability level.

Table 2. Interatomic distances [Å] for the hydrogen bonds in compound **I**.

	$\text{O}_\text{W} \cdots \text{O}^{[\text{a}]}$	$\text{O}-\text{H}^{[\text{b}]}$	$\text{H} \cdots \text{O}^{[\text{b}]}$	$\cdots \text{O}=\text{P}^{[\text{a}]}$
Cation 1				
$\text{O1W}-\text{H} \cdots \text{O5}$	2.489(4)	1.09	1.40	1.497(3)
$\text{O1W}-\text{H} \cdots \text{O7}$	2.461(4)	1.11	1.35	1.494(3)
$\text{O1W}-\text{H} \cdots \text{O8}$	2.518(5)	1.11	1.40	1.491(3)
Cation 2				
$\text{O2W}-\text{H} \cdots \text{O1}$	2.470(6)	1.17	1.30	1.495(4)
$\text{O2W}-\text{H} \cdots \text{O2}$	2.486(5)	1.12	1.37	1.495(3)
$\text{O2W}-\text{H} \cdots \text{O3}$	2.478(5)	1.11	1.37	1.504(3)
Cation 3				
$\text{O3W}-\text{H} \cdots \text{O4}$	2.481(5)	1.11	1.38	1.491(3)
$\text{O3W}-\text{H} \cdots \text{O6}$	2.487(5)	1.09	1.40	1.502(3)
$\text{O3W}-\text{H} \cdots \text{O9}$	2.492(5)	1.12	1.37	1.489(3)

[a] Values obtained from crystal structure determination. [b] Values estimated from NMR spectroscopic data (no corrections for the  $\text{H}_3\text{O}$  librations were made).

$\text{O}-\text{H} \cdots \text{O}$  bonds, we estimated the proton positions in the hydrogen bonds. On the whole, the obtained proton arrangement (Table 2) corresponds to asymmetrical H-bonding with the mean distances of 1.11(2) and 1.37(3) Å for  $\text{O}_\text{W}-\text{H}$  and  $\text{H} \cdots \text{O}$ , respectively, which are in satisfactory agreement with the experimental correlation of  $\text{O}-\text{H}$  vs.  $\text{H} \cdots \text{O}$  found for the oxonium ions in inorganic crystals.<sup>[16]</sup> Therefore, the discussed complex ion can be named *tris(oxotriphenylphosphane)oxonium*.

The complex  $[\text{H}_3\text{O}(\text{Ph}_3\text{PO})_3]_2[\text{Mo}_6\text{Cl}_{14}]$  is brightly luminescent in the red and near infrared regions of the emission spectrum (Figure 5). It is interesting to note that the intensity of its emission is almost twice as high as that for the initial compound  $(\text{H}_3\text{O})_2\text{Mo}_6\text{Cl}_{14} \cdot 6\text{H}_2\text{O}$ . Recently we observed similar luminescence behaviour in some related complexes  $[\text{Ca}(\text{DMF})_6][\text{Mo}_6\text{Cl}_{14}]$  and  $[\text{Ca}(\text{Ph}_3\text{PO})_4][\text{Mo}_6\text{Cl}_{14}]$ ;<sup>[15]</sup> the emission intensities for these two complexes are four and six times higher than that for  $(\text{H}_3\text{O})_2\text{Mo}_6\text{Cl}_{14} \cdot 6\text{H}_2\text{O}$ .

We tried to find a similar cationic complex ion (as in **I**) in the related rhenium system containing the isoelectronic cluster complex  $[\text{Re}_6\text{S}_6\text{Br}_8]^{2-}$  with similar geometric characteristics. The interaction of the rhenium complex  $\text{K}_2\text{Re}_6\text{S}_6\text{Br}_8$  with triphenylphosphane oxide was carried out in acetonitrile solution with the addition of several drops of  $\text{HBr}$ . Indeed, we succeeded in obtaining a similar complex

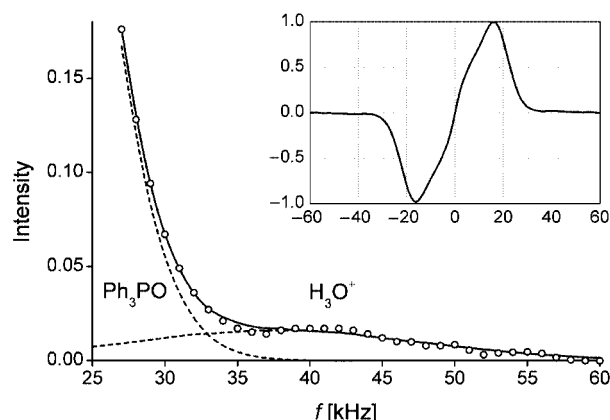


Figure 4. Fragment of the  $^1\text{H}$  NMR absorption derivative for  $[\text{H}_3\text{O}(\text{Ph}_3\text{PO})_3]_2[\text{Mo}_6\text{Cl}_{14}]$  at 180 K (O) (the complete spectrum is illustrated in the inset). The best fit to the experimental spectrum is shown as a solid line. The dashed curves correspond to the contributions of the  $\text{H}_3\text{O}^+$  and the  $\text{Ph}_3\text{PO}$  protons.

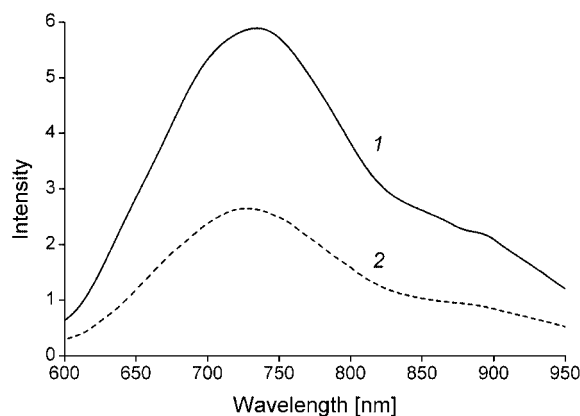


Figure 5. Luminescence spectrum of  $[\text{H}_3\text{O}(\text{OPPh}_3)_3]_2[\text{Mo}_6\text{Cl}_{14}]$  (1) and  $(\text{H}_3\text{O})_2\text{Mo}_6\text{Cl}_{14} \cdot 6\text{H}_2\text{O}$  (2).

$[\text{H}_3\text{O}(\text{Ph}_3\text{PO})_3]_2[\text{Re}_6\text{S}_6\text{Br}_8]$  (**III**) with unit-cell parameters [ $a = 13.699(3)$  Å,  $b = 22.731$  Å,  $c = 29.596(5)$  Å,  $a = 102.889(8)^\circ$ ,  $\beta = 99.129(5)^\circ$ ,  $\gamma = 92.202(5)^\circ$ ] similar to those observed for **I** (Table 1). Unfortunately, compound **III** crystallized with a very small yield, and several crystals that were isolated had poor quality and were therefore unsuitable for single-crystal X-ray analysis.

In the  $\text{K}_2\text{Re}_6\text{S}_6\text{Br}_8-\text{Ph}_3\text{PO}-\text{HBr}$  system, another new complex with the composition  $[\text{H}(\text{Ph}_3\text{PO})_2]_2[\text{Re}_6\text{S}_6\text{Br}_8]$  (**II**) was obtained in a high yield (Table 1, Figure 6). In **II**, there are two types of cluster anions,  $[\text{Re}_6\text{S}_2(\text{S}_{2/3}\text{Br}_{1/3})_6\text{Br}_6]^{2-}$  and  $[\text{Re}_6\text{S}_4(\text{S}_{1/2}\text{Br}_{1/2})_4\text{Br}_6]^{2-}$ , with different distributions of the  $\mu_3$  ligands (Figure 7). In  $[\text{Re}_6\text{S}_2(\text{S}_{2/3}\text{Br}_{1/3})_6\text{Br}_6]^{2-}$ , four sulfur and two bromine atoms alternatively occupy six corners of a cube; in  $[\text{Re}_6\text{S}_4(\text{S}_{1/2}\text{Br}_{1/2})_4\text{Br}_6]^{2-}$ , two sulfur and two bromine atoms are distributed over four positions. The interatomic distances for both isomers are summarized in Table 3. The observation of similar cluster isomers among octahedral cluster complexes is not unexpected. In particular, it was shown<sup>[17]</sup> that in the related complex  $[\{\text{Re}_6\text{Se}_6\text{Br}_2\}\text{Br}_6]^{2-}$ , the cluster core  $[\text{Re}_6\text{Se}_6\text{Br}_2]^{4+}$  is repre-

sented by three isomers that can be identified in solution by  $^{77}\text{Se}$  NMR spectroscopy.

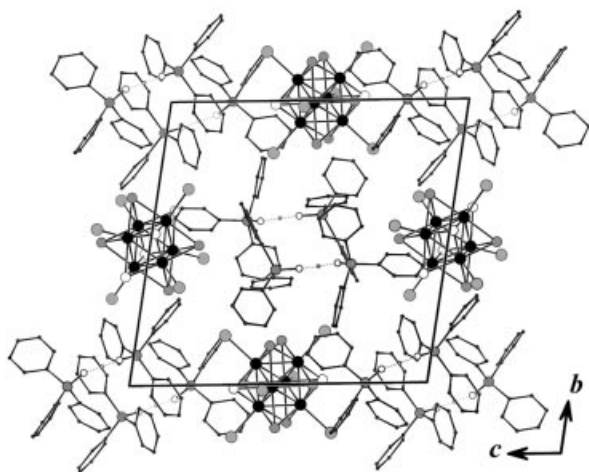


Figure 6. Packing in the crystal structure of  $[\text{H}(\text{Ph}_3\text{PO})_2]_2\text{-}[\text{Re}_6\text{S}_6\text{Br}_8]$ .

In compound **II**, the triphenylphosphane oxide molecules are integrated into H-bonded dimers  $[\text{H}(\text{OPPh}_3)_2]^+$  (Figure 8) with very short O–O distances of 2.34(1) Å and 2.41(1) Å for the two structurally nonequivalent dimers in the unit cell. Note that one of these distances is even less than the known limit (2.39 Å) usually associated with the formation of the symmetric O–H–O bond.<sup>[16]</sup> The P=O bond lengths are essentially different in each of the dimers: 1.483(8) and 1.549(7) Å, 1.488(10) and 1.523(8) Å. This difference might possibly be explained by the asymmetric proton positions in the hydrogen bonds, i.e. the protons are shifted from the bond centres towards the oxygen atoms with longer P=O contacts.<sup>[9]</sup> In this regard, of interest is the MAS  $^1\text{H}$  NMR spectrum (Figure 9): the protons involved in H-bond formation give rise to a diffuse peak with a chemical shift  $\delta$  of 17.5(5) ppm. The observed  $\delta$  value differs noticeably from the shift of 21.6 ppm expected for a symmetrical bond.<sup>[18]</sup> On the basis of the various experimental correlations between the chemical shift and hydrogen-bond geometry,<sup>[18,19]</sup> the proton displacements from the bond

Table 3. Bond lengths [Å] in the cluster anions  $[\text{Re}_6\text{S}_6\text{Br}_8]^{2-}$  of compound **II**.<sup>[a]</sup>

$[\text{Re}_6\text{S}_2(\text{S}_{2/3}\text{Br}_{1/3})_6\text{Br}_6]^{2-}$		$[\text{Re}_6\text{S}_4(\text{S}_{1/2}\text{Br}_{1/2})_4\text{Br}_6]^{2-}$	
<b>Re–Re</b>		<b>Re–Re</b>	
Re(1)–Re(2)	2.5978(5)	Re(4)–Re(6)#2	2.5959(6)
Re(1)–Re(2)#1	2.6101(6)	Re(4)–Re(6)	2.5964(6)
Re(1)–Re(3)#1	2.6112(6)	Re(4)–Re(5)	2.6005(6)
Re(1)–Re(3)	2.5929(6)	Re(4)–Re(5)#2	2.6055(5)
Re(2)–Re(3)#1	2.6114(6)	Re(6)–Re(5)#2	2.5886(6)
Re(2)–Re(3)	2.5996(6)	Re(6)–Re(5)	2.6071(5)
<b>Re–S</b>		<b>Re–S</b>	
Re(1)–S(1)	2.408(3)	Re(4)–S(6)	2.454(2)
Re(2)–S(1)	2.416(3)	Re(4)–S(7)	2.455(2)
Re(3)–S(1)	2.407(3)	Re(5)–S(6)#2	2.440(2)
<b>Re–Q<sup>i</sup> (S, Br)</b>		<b>Re–Q<sup>i</sup> (S, Br)</b>	
Re(1)–Q(2)	2.498(2)	Re(5)–S(7)	2.434(3)
Re(1)–Q(3)	2.5226(19)	Re(6)–S(6)	2.447(3)
Re(1)–Q(4)	2.522(2)	Re(6)–S(7)#2	2.447(2)
Re(2)–Q(2)#1	2.493(2)	<b>Re–Q<sup>i</sup> (S, Br)</b>	
Re(2)–Q(3)	2.536(2)	Re(4)–Q(5)	2.493(2)
Re(2)–Q(4)#1	2.510(2)	Re(4)–Q(8)	2.514(2)
Re(3)–Q(2)	2.478(2)	Re(5)–Q(5)	2.507(2)
Re(3)–Q(3)#1	2.5297(19)	Re(5)–Q(8)#2	2.511(2)
Re(3)–Q(4)#1	2.5006(19)	Re(6)–Q(5)	2.521(2)
<b>Re–Br</b>		Re(6)–Q(8)#2	2.522(2)
Re(1)–Br(1)	2.5234(11)	<b>Re–Br</b>	
Re(2)–Br(5)	2.5368(12)	Re(4)–Br(9)	2.5358(13)
Re(3)–Br(6)	2.5401(13)	Re(5)–Br(10)	2.5336(11)
		Re(6)–Br(11)	2.5180(13)

[a] Symmetry transformations used to generate equivalent atoms: #1  $-x+1, -y, -z+1$ ; #2  $-x+1, -y-1, -z$ .

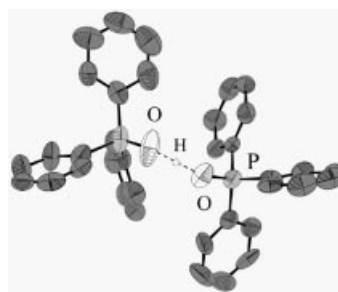


Figure 8. The structure of cation  $[(\text{Ph}_3\text{PO})_2\text{H}]^+$  in compound **II**. Displacement ellipsoids are drawn at the 50% probability level.

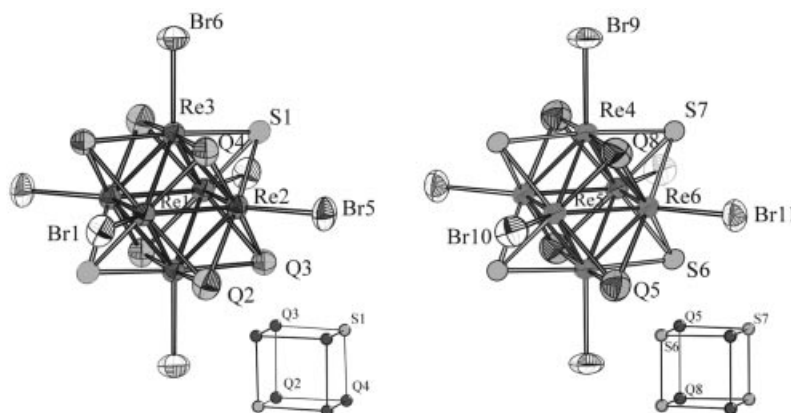


Figure 7. The structures of the cluster anions  $[\text{Re}_6\text{S}_6\text{Br}_8]^{2-}$  in compound **II**. Q – mixed S/Br positions. Displacement ellipsoids are drawn at the 50% probability level.



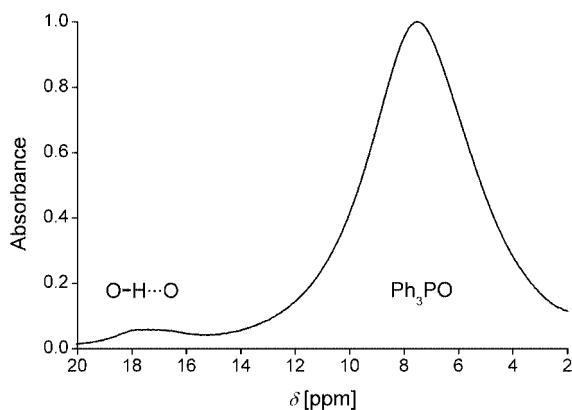


Figure 9. MAS  $^1\text{H}$  NMR spectrum of  $[\text{H}(\text{Ph}_3\text{PO})_2]_2[\text{Re}_6\text{S}_6\text{Br}_8]$ .

centre were estimated to fall in the range from 0.13 to 0.17 Å.

The obtained experimental results together with those cited in the literature allow us to predict that triphenylphosphane oxide in acid solutions is able to form several protonated complex ions, namely  $[\text{HOPPh}_3]^+$ ,  $[\text{H}(\text{OPPh}_3)_2]^+$ ,  $[(\text{H}_3\text{O})(\text{OPPh}_3)_2]^+$  and  $[(\text{H}_3\text{O})(\text{OPPh}_3)_3]^+$ , which can exist simultaneously in chemical equilibrium with each other. The question “What forms can be isolated in proper complexes?” can be answered differently depending on the specific chemical system to be studied. The oxonium ion  $\text{H}_3\text{O}^+$  plays a key role in the formation of cationic trimeric complex ion  $[\text{H}_3\text{O}(\text{OPPh}_3)_3]^+$  (a single proton involved in the formation of  $[\text{HOPPh}_3]^+$  or  $[\text{H}(\text{OPPh}_3)_2]^+$  is obviously not able to interact with a third oxygen atom). In solids containing  $\text{OPPh}_3$  and large cluster anions, we have discovered the cationic complex ion  $[\text{H}(\text{OPPh}_3)_2]^+$  (observed earlier<sup>[9]</sup>) and a novel complex ion  $[\text{H}_3\text{O}(\text{OPPh}_3)_3]^+$ . These complex ions resemble well-known protonated complexes inherent to hydrated systems (Zundel complex  $[\text{H}_5\text{O}_2]^+$ <sup>[20]</sup> and Eigen complex  $[\text{H}_9\text{O}_4]^+$ <sup>[21]</sup> in which the  $\text{H}_2\text{O}$  molecules are replaced by  $\text{OPPh}_3$ ) owing to the type of solvation observed in these complexes.

## Experimental Section

**Materials and Methods:** Starting compounds were prepared by known methods described in the literature.  $\text{Mo}_6\text{Cl}_{12}$  was synthesized by the method described previously.<sup>[22]</sup>  $(\text{H}_3\text{O})_2\text{-Mo}_6\text{Cl}_{14}\cdot 6\text{H}_2\text{O}$  was prepared by dissolution of  $\text{Mo}_6\text{Cl}_{12}$  in hot concentrated  $\text{HCl}$ . The solution was filtered and  $(\text{H}_3\text{O})_2\text{-Mo}_6\text{Cl}_{14}\cdot 6\text{H}_2\text{O}$  was crystallized by cooling of the solution. The precipitate was washed with cold water and dried in air.  $\text{K}_2[\text{Re}_6\text{S}_6\text{Br}_8]$  was synthesized as described previously.<sup>[23]</sup> Other reagents were purchased from Aldrich and used as received without additional treatment. Elemental analyses (Carlo Erba Instrument EA1106) were performed by the laboratory of microanalysis at the Vorozhtsov Institute of Organic Chemistry, Siberian Branch of Russian Academy of Sciences.

**Synthesis of  $[\text{H}_3\text{O}(\text{Ph}_3\text{PO})_3]_2[\text{Mo}_6\text{Cl}_{14}]$  (I):**  $(\text{H}_3\text{O})_2\text{-Mo}_6\text{Cl}_{14}\cdot 6\text{H}_2\text{O}$  (100 mg, 0.08 mmol) was dissolved in acetonitrile (10 mL), and  $\text{Ph}_3\text{PO}$  (300 mg, 1.1 mmol) was dissolved in acetonitrile (10 mL). The solutions obtained were mixed, boiled for 5 min and evapo-

rated until a crystalline precipitate began to form. Then the solution was cooled. The crystals were filtered and washed with diethyl ether (5 mL). Yield: 170 mg (61%). Single crystals for X-ray diffraction analysis were separated from the precipitate. The XPD pattern of solid **I** agreed well with the pattern calculated from the single-crystal parameters.  $\text{C}_{108}\text{H}_{96}\text{Cl}_{14}\text{Mo}_6\text{O}_8\text{P}_6$  (2779.61): calcd. C 46.67, H 3.48; found C 46.61, H 3.60%.

**Synthesis of  $[\text{H}(\text{Ph}_3\text{PO})_2]_2[\text{Re}_6\text{S}_6\text{Br}_8]$  (II):**  $\text{K}_2\text{Re}_6\text{S}_6\text{Br}_8$  (100 mg, 0.04 mmol) was dissolved in acetonitrile (10 mL), and  $\text{Ph}_3\text{PO}$  (100 mg, 0.36 mmol) was dissolved in acetonitrile (10 mL). The solutions obtained were mixed, a drop of  $\text{HBr}$  was added and the solution boiled for 2–3 min. The solution was filtered, and the filtrate was evaporated to a volume of 10 mL, after which diffusion was carried out using ether. Bright red vinous crystals precipitated, which were collected. Single crystals for X-ray diffraction analysis were separated from the precipitate manually. Yield 95 mg (63%). A further amount of the compound could be obtained from the mother liquor by evaporation. The XPD pattern of solid **II** agreed with the pattern calculated from the single-crystal parameters.  $\text{C}_{72}\text{H}_{62}\text{Br}_8\text{O}_4\text{P}_4\text{Re}_6\text{S}_6$  (3063.94): calcd. C 28.22, H 2.04; found C 28.39, H 2.18%.

**Crystallography:** The structures of complexes **I** and **II** were solved by X-ray diffraction analysis of single crystals. The diffraction data were collected on a Bruker-Nonius X8APEX CCD diffractometer by using  $\text{Mo-K}_\alpha$  (0.71073 Å) radiation and a graphite monochromator. The absorption corrections were semiempirical using the intensities of equivalent reflections and the SADABS software.<sup>[24]</sup> The structures were solved by direct methods and refined by full-matrix least-squares on  $F^2$ ; anisotropic approximation for non-hydrogen atoms using the program package SHELXL.<sup>[25]</sup> The crystallographic and experimental details are given in Table 1. CCDC 614149 (**I**) and 614150 (**II**) contain the supplementary crystallographic data for this paper. These data can be obtained free of charge from The Cambridge Crystallographic Data Centre via [www.ccdc.cam.ac.uk/data\\_request/cif](http://www.ccdc.cam.ac.uk/data_request/cif).

**NMR Spectroscopy:** MAS  $^1\text{H}$  NMR measurements for **II** were performed at room temperature with a Bruker Avance 400 spectrometer at 400.13 MHz. The  $\pi/2$  rf-pulse width and the recycle delay were 10  $\mu\text{s}$  and 60 s, respectively. The spectra were recorded at rotation frequencies in the range 10–20 kHz using a 4-mm  $\text{ZrO}_2$  rotor. The powder sample was prepared by several synthesis cycles described above. The  $^1\text{H}$  chemical shift was measured relative to the resonance of TMS. The wide-line  $^1\text{H}$  NMR spectrum of **I** was recorded in the form of the first derivative of the NMR absorption line by sweeping the frequency in the neighbourhood of 25 MHz in the temperature range 180–350 K with a home-made NMR spectrometer with signal accumulation. For the analyzed spectra, the signal/noise ratio reached about  $3 \times 10^3$ . The  $\text{H}_3\text{O}^+$  spectra, as a function of the proton–proton distances  $r_1$ ,  $r_2$  and  $r_3$ , were simulated with a known three-spin approximation.<sup>[26,27]</sup> The contribution of the aromatic protons in the analyzed frequency region was approximated by a rectangle-Gaussian convolution function<sup>[28]</sup> determined by two parameters:  $a$  and  $b$  for the rectangle and Gaussian, respectively. This gives the NMR absorption derivative for a powder in the form:

$$F(f) \sim -c/(4\pi\beta^3) \int \sum J_i(f - \delta_i) \exp[-(f - \delta_i)^2/2\beta^2] d\Omega \\ + (1 - c)/(2ab) \{ \exp[-(f + a)^2/2b^2] - \exp[-(f - a)^2/2b^2] \}$$

where  $J_i$  and  $\delta_i$  are corresponding intensities and line positions of the  $\text{H}_3\text{O}^+$  NMR septet,<sup>[27]</sup> which depend on  $r_i$  and the orientation ( $\Omega$ ) of the proton triangle with respect to the external magnetic field;  $\beta$  is the parameter of the spectral broadening due to the di-

polar interactions of the  $\text{H}_3\text{O}^+$  group with surrounding protons;  $c$  is the concentration of the  $\text{H}_3\text{O}^+$  protons. In the frequency ranges  $|\Delta f| = (25 - 60)$  kHz, the discrepancy between the experimental spectra and the best fits obtained with this equation is about 2.5%.

**Luminescence Spectroscopy:** Luminescence spectra were recorded at room temperature by using the spectrometer SDL-1 with the photoelectron multiplier PEM-62. The excitation source was a mercury lamp of type DRSH-250 with a 365-nm filter. The measured samples had the shape of square pellets of equal size.

## Acknowledgments

This work was supported by the Russian Foundation for Basic Research, projects no. 05-03-32123, 05-03-08090 and 06-03-89503-HHC. The authors thank Prof. O. Lapina and Dr. K. Romanenko for recording MAS  $^1\text{H}$  NMR spectra.

- [1] D. Hadzi, *J. Chem. Soc.* **1962**, 5128–5138.
- [2] D. Thierbach, F. Huber, *Z. Anorg. Allg. Chem.* **1979**, 451, 137–142.
- [3] H. J. Haupt, F. Huber, C. Kruger, H. Preut, D. Thierbach, *Z. Anorg. Allg. Chem.* **1977**, 436, 229–236.
- [4] H. P. Lane, C. A. McAuliffe, R. G. Pritchard, *Acta Crystallogr., Sect. C* **1992**, 48, 2002–2004.
- [5] L. Golic, V. Kaucic, *Cryst. Struct. Commun.* **1976**, 5, 319–324.
- [6] D. Thierbach, F. Huber, *Z. Anorg. Allg. Chem.* **1979**, 457, 189–196.
- [7] J. P. Declercq, G. Germain, J. P. Putzeys, S. Rona, M. van Meerssche, *Cryst. Struct. Commun.* **1974**, 3, 579–582.
- [8] P. G. Jones, G. M. Sheldrick, *Acta Crystallogr., Sect. B* **1978**, 34, 1353–1355.
- [9] M. Yu. Antipin, A. E. Kalinin, Yu. T. Struchkov, E. I. Matrosov, M. I. Kabachnik, *Kristallografiya* **1980**, 25, 514–524 (in Russian).
- [10] J. A. Thomas, T. A. Hamor, *Acta Crystallogr., Sect. C* **1993**, 49, 355–357.
- [11] J. C. Sheldon, *J. Chem. Soc.* **1961**, 750–752.
- [12] W. Preetz, G. Peters, D. Bublit, *Chem. Rev.* **1996**, 96, 977–1025.
- [13] N. Prokopuk, D. F. Shriver, *Adv. Inorg. Chem.* **1999**, 46, 1–49.
- [14] T. G. Gray, *Coord. Chem. Rev.* **2003**, 243, 213–235.
- [15] Z. S. Kozhomuratova, Y. V. Mironov, M. A. Shestopalov, Ya, M. Gaifulin, N. V. Kutatieva, E. M. Uskov, V. E. Fedorov, *Russ. J. Coord. Chem.* **2007**, 33, 1–6.
- [16] Th. Steiner, W. Saenger, *Acta Crystallogr., Sect. B* **1994**, 50, 348–357.
- [17] S. S. Yarovoi, S. F. Solodovnikov, S. V. Tkachev, Yu. V. Mironov, V. E. Fedorov, *Russ. Chem. Bull.* **2003**, 52, 68–72.
- [18] Th. Emmeler, S. Gieschler, H. H. Limbach, G. Buntkowsky, *J. Mol. Struct.* **2004**, 700, 29–38.
- [19] E. Brunner, U. Sternberg, *Prog. Nucl. Magn. Reson. Spectrosc.* **1998**, 32, 21–57.
- [20] G. Zundel, H. Metzger, *Z. Phys. Chem., Neue Folge* **1968**, 58, 225–245.
- [21] E. Wicke, M. Eigen, T. Ackerman, *Z. Phys. Chem., Neue Folge* **1954**, 1, 340–364.
- [22] A. V. Nikolaev, A. A. Opalovsky, V. E. Fedorov, in *Thermal Analysis*, Academic Press. Inc. New York, **1969**, vol. 2, p. 793–810.
- [23] A. Slougui, S. Ferron, A. Perrin, M. Sergent, *J. Cluster Sci.* **1997**, 8, 349–359.
- [24] *SADABS* (Version 2.11), Bruker Advanced X-ray Solutions, Bruker AXS Inc., Madison, Wisconsin, USA, **2004**.
- [25] *SHELXTL* (Version 6.12), Bruker Advanced X-ray Solutions, Bruker AXS Inc., Madison, Wisconsin, USA, **2004**.
- [26] E. R. Andrew, B. Bersohn, *J. Chem. Phys.* **1950**, 18, 159–161.
- [27] E. R. Andrew, N. D. Finch, *Proc. Phys. Soc.* **1957**, 70B, 980–990.
- [28] A. Abragam, *The Principles of Nuclear Magnetism*, Clarendon Press, Oxford, **1961**.

Received: December 8, 2006  
Published Online: March 30, 2007